Mol. Cryst. Liq. Cryst., Vol. 387, pp. [263]/39–[274]/50

1058-725X/02 $12.00 + .00
DOI: 10.1080/10587250290113547

GRAPHITIC CONES IN CARBON NANOFIBRES

H. Terrones, M. Muñoz-Navia, and M. Terrones
IPICyT, Venustiano Carranza 2425-A,
Col. Los Filtros, 78210 San Luis Potosí, SLP, México

T. Hayashi, Y. A. Kim, and M. Endo
Shinshu University, Faculty of Engineering, Wakasato,
Nagano-city, 380-8553, Japan

M. Muñoz-Navia and J. Dorantes-Dávila
Instituto de Física "Manuel Sandoval Vallarta",
UASLP, 78000 San Luis Potosí, SLP, México

M. Terrones and N. Grobert
Fullerene Science Centre, CPES, University of Sussex,
Brighton BN1 9QJ, UK

R. Kamalakaran
Max-Planck-Institute für Metallforschung, Seestr. 92,
Stuttgart D 70174, Germany

R. Escudero
Instituto de Investigaciones en Materiales, UNAM,
A.P.70-360, 01000 México, D.F., México

M. S. Dresselhaus
Massachusetts Institute of Technology, Cambridge,
Massachussetts 02139-4307, USA

The authors are grateful to Ph. Redlich, M. Rühle and K. Labitzke for stimulating discussions and technical assistance. HT acknowledges the support of the Japanese Society for the Promotion of Science (JSPS grant No. S-00247) and the hospitality of Shinsu University, Japan, where he has been a visiting scientist. MT and HT are grateful to CONACYT-México grant W-8001-millenium initiative and grants 32085-E, 36365, MMN and JDD acknowledge IMP-Mexico grant FIES-98-101-I, CONACYT grant 37589-U and MMN thanks CONACyT-México for the PhD grant.

High yields of graphitic conical nanofibres (5–70 nm OD; <5 μm in length) are produced by pyrolysing various palladium precursors under an Ar atmosphere at 850–1000°C. The fibres exhibit diamond-shaped Pd particles at their tips, which are responsible for the carbon aggregation and its subsequent diffusion. This carbon replication phenomenon on the Pd particles results in the formation of stacked graphene cones, which grow aligned along a common axis, thus creating graphitic nanofibres. The cones within the fibres can be either open (lamp-shade type) or closed. The material has been analysed using sophisticated electron microscopy (HRTEM, SEM, ED) and spectroscopic techniques (Raman, EELS, EDX). Due to the large number of open edges, we envisage that these novel nanofibres may find important applications in the fabrication of field emitters, gas storage devices and composites.

Keywords: nanocones; nanotubes; carbon; palladium

INTRODUCTION

The identification of carbon nanotubes (CNTs) [1] has propelled a new area of carbon nanomaterials, which is expected to have important implications for the development of emerging technologies such as the fabrication of electronic devices, flat panel displays, robust composites, nano-switches, etc. [2–6]. These results prove that carbon is very flexible and is able to form not only CNTs (multi- or single-walled), but also fullerenes [7], graphitic onions [8], toroids [9], boxes [10], and cones [11–13]. In this paper we report a simple route to synthesize a new type of graphitic conical nanofibre by pyrolysing solid Pd compounds. Our results also demonstrate that Pd can be used as an efficient catalyst for the formation of carbon nanostructures.

The graphitic cones in our fibres exhibit apex angles from 32° to 82°, which can be explained in terms of open conical graphene sheets (lamp-shade type) and have not been considered hitherto. According to theoretical calculations, closed graphene cones exhibit a charge transfer to the pentagonal rings (caps) [14], which could be important in the development of field emission sources. However, open cones may exhibit enhanced field emission properties (caused by the open edge sites) as well as Aharonov-Bohm magnetic effects and magnetoconductance [15]. We believe that localised states close to the Fermi level (for the open cones) may give rise to materials with novel electronic and magnetic properties [16–17].

EXPERIMENTAL

The pyrolysis of Pd precursors was carried out in the presence of Ar using a two stage furnace system coupled with temperature controllers [18].

Powders (10–50 mg) of palladium acetyl-acetonate ($[CH_3COCH=C(O)CH_3]_2Pd$, Aldrich 99%), palladium acetate ($[CH_3CO_2]_2Pd$, Aldrich 98%), or dichloro (1,5-cyclooctadiene) palladium ($C_8H_{12}Cl_2Pd$, Aldrich 99%), were inserted in one end of a quartz tube (80 cm long; 6 mm id). Subsequently, the tube was placed in a two stage furnace and the region containing the powder sample was located outside the furnaces. Ar flows (5–15 cm^3/min) were then passed through the tube and the two furnaces were heated (50°C/min) to the set temperature (from 450°C to 1050°C in 100°C steps). At this temperature, the tube was shifted so that the region containing the powder was introduced into the first furnace region. This promoted a fast (<10 sec) reaction, which caused the deposition of carbonaceous materials in the first and second furnaces. The furnaces were left operating for an additional 15 min in order to anneal the products (see Fig. 1).

Deposits scratched from the tube walls (both furnaces) were then analysed using scanning electron microscopy (SEM; JEOL JSM-6335F operating at 3–15 kV and a Zeiss DSM 982 Gemini operated at 1–2 kV). Minute amounts of the powder samples (1–2 mg) were then dispersed ultrasonically (5–30 min) in 5 ml acetone, and few drops of the dispersions were placed on a holey carbon grid for transmission electron microscopy studies. High resolution transmission electron microscopy (HRTEM) measurements were carried out in a JEOL JEM-2010FEF operated at 200 kV (equipped with an omega filter, a Gatan multiscan camera and an energy dispersive X-ray -EDX-Oxford Ins. detector), a JEOL JEM-4000 microscope operating at 400 kV and a JEOL JEM-3000F microscope operated at 300 kV (equipped with an EDX Noran Inst. detector).

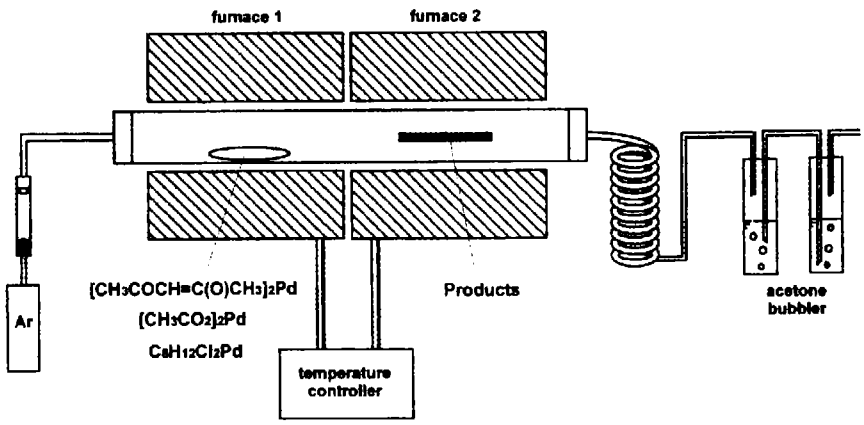

FIGURE 1 Experimental set up for the production of graphitic-conical nanofibres.

Raman spectra were recorded at room temperature under ambient conditions using a Renishaw Raman Image Microscope System 1000 equipped with a CCD multi-channel detector. The excitation source consisted of an Ar-ion laser (514.5 nm). The laser beam (0.8 μm spot size) was focused on the sample using an optical microscope (objective lens of ×100). During spectra acquisition, the optical power was maintained at 5 mW in order to avoid any signal shifts of the spectra and sample damage caused by local overheating. The scattered light was collected in a back-scattering configuration. The peak frequencies of the Raman spectra were determined by fitting the raw data with a Lorentzian distribution function. The Raman spectral lines were obtained with an accuracy better than $\pm 2\,cm^{-1}$.

RESULTS AND DISCUSSION

SEM and TEM studies reveal that the material collected from the furnace consists of entangled nanofibres exhibiting "conical-shape" metal particles at their tips (Fig. 2). These fibres seem to grow radially from a common central site (Fig. 2b). From TEM observations, we find Pd multiple-twinned clusters (some of them with decahedral shapes), surrounded by disordered graphite layers. We commonly observe regions in which these Pd twin nanocrystals fragment into "diamond-shape" particles. Electron diffraction (ED) patterns from these decahedral twinned particles exhibit five-fold symmetry containing the (111) ($d_{111} = 2.24$ Å) and (002) ($d_{002} = 1.94$ Å) Pd planes, with the [110] direction being the zone axis (Figs. 2e, 2f, 5c and 5d).

The fibres exhibit diameters ranging from 5 nm to 70 nm and lengths up to 5 μm. TEM observations revealed that all the fibres exhibit stacked-cone morphologies (Figs. 2, 4 and 5) with a Pd particle (detected by EDX and electron diffraction), which is firmly attached at the tip, even after a 30 minute sonication treatment.

The cone angles within different fibres have been measured by ED, and taking the fast Fourier transform (FFT) of several micrographs. We observed that angles between 32° and 82° were mainly present. It is important to mention that angles around 40°, 60° and 80° might correspond to 240°, 180° and 120° disclinations in graphite [19], respectively. From a theoretical stand point, graphene closed cones can be generated by introducing n = 1 to 5 pentagonal carbon rings within the hexagonal framework. Using this definition, symmetric cones exhibit angles given by: $\theta = 2^*\ \arcsin(1-n/6) = 112.8°$, 83.62°, 60°, 38.94° and 19.188°. However, angles at *ca.* 30°, 50° and 70°, forbidden by the closed cone approach [12], can only be explained in terms of an open cone model. Thus, with an open apex, the cone becomes less rigid and more possibilities for conical

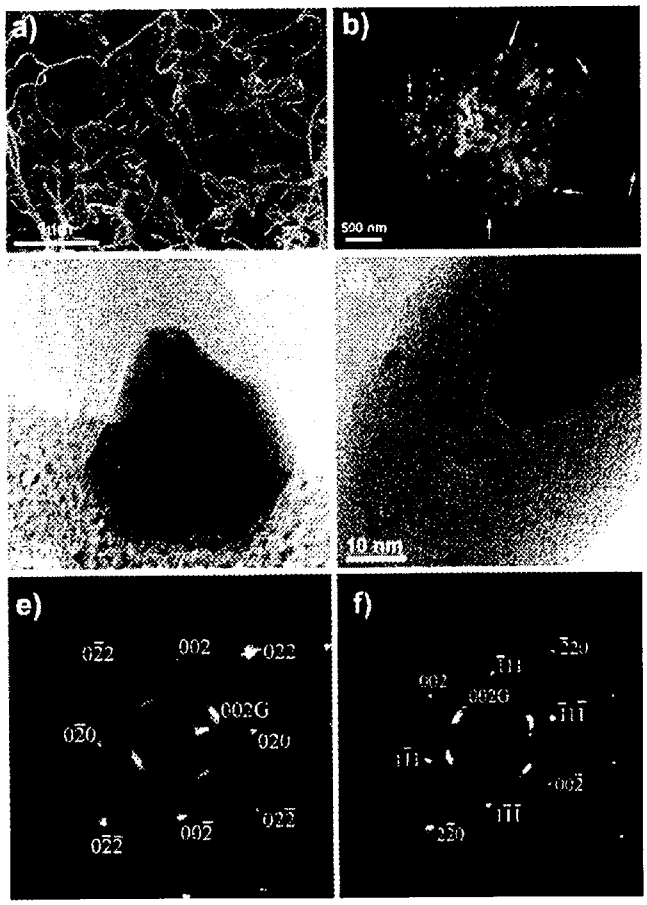

FIGURE 2 (a) SEM images of entangled Pd grown carbon nanofibres (the scale correspond to 1 μ); (b) SEM image of nanofibres in which the arrows show conical Pd particles at the tips; (c) and (d) HRTEM images of typical Pd particles located at the tip of the fibres (note the conical arrangement of graphene layers); (e) and (f) Electron diffraction (ED) patterns of the conical fibres close to the Pd tip particle. In (e) the Pd zone axis is [100], whereas in (f) the zone axis is [110].

graphitic geometries can be envisaged such as the great variety of chiral configurations (Fig. 3).

Once the open cones are formed, their closure can be achieved by introducing defects such as pentagons. In our fibres, if the cones are closed, it is likely that the final closure occurs at the apex. Therefore, the open cone approach supports the formation of our structures and explains the variety of angles observed (Fig. 4).

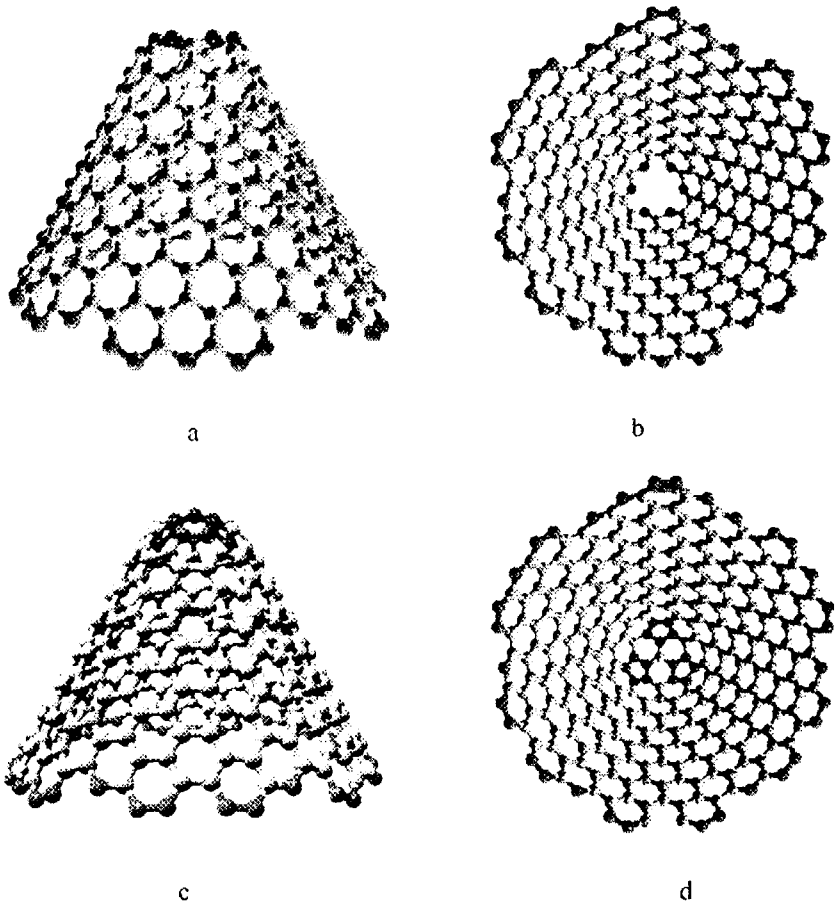

FIGURE 3 Open graphitic cone a) Side view, b) Top view. Closed graphitic cone with pentagons c) Side view d) Top view. Important properties are expected from the edges and the open tip (See Color Plate IV).

It is commonly observed that at the opposite end of the conical fibres (opposite to the Pd triangular-shaped particle at the tip), Pd clusters of round (not triangular) morphologies appear. This observation suggests that the carbon fragmentation/precipitation, and fibre growth only occurs on the triangular (conical) Pd particles. Moreover, broken nanofibres exhibiting closed conical arrangements at the fibre ends (opposite to the Pd triangular particle; Fig. 5) are also observed. From high resolution TEM images, we notice that the graphite cones always adopt the shape of the conical catalyst particles.

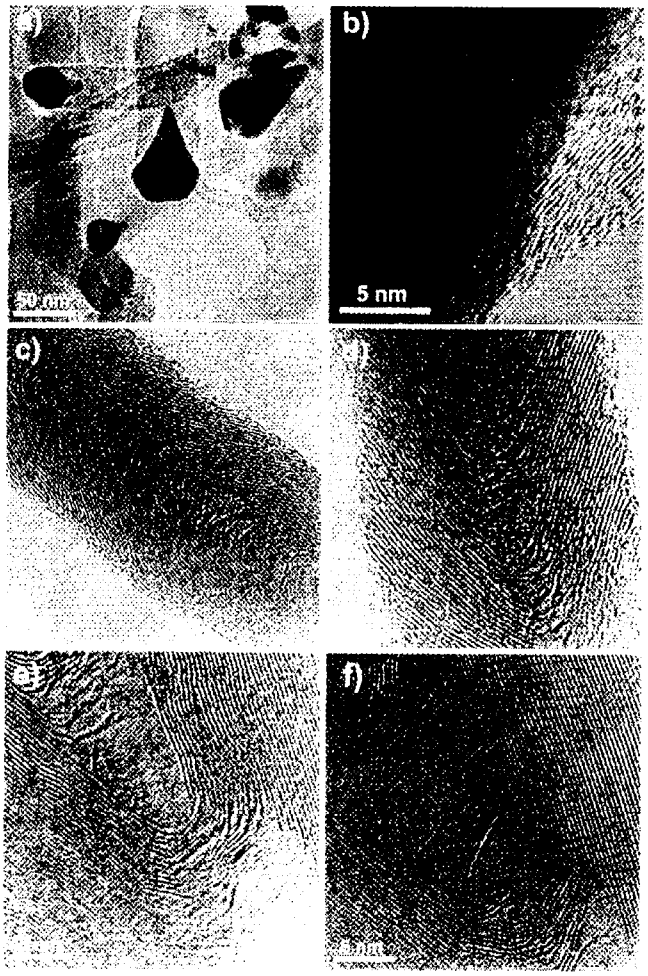

FIGURE 4 (a) TEM image of various conical nanofibres exhibiting "diamond-shape" Pd particles at the tips; (b) HRTEM image of an individual fibre tip showing the Pd [100] and the graphite [002] planes, note that these planes do not show a clear epitaxial correlation; (c)–(f) HRTEM images of Pd grown nanofibres exhibiting different conical morphologies. Note that the degree of graphitisation differs from fibre to fibre. The tips of the individual cones are frequently ill-formed, and occasionally the cones are open.

According to our observations, the following growth scenario (see Fig. 6) can be proposed: (i) At 850°C, Pd and carbon clusters form; (ii) Pd clusters aggregate in order to create multiple-twinned particles (see also Fig. 5d), which can be either decahedral or icosahedral; (iii) carbon species interact

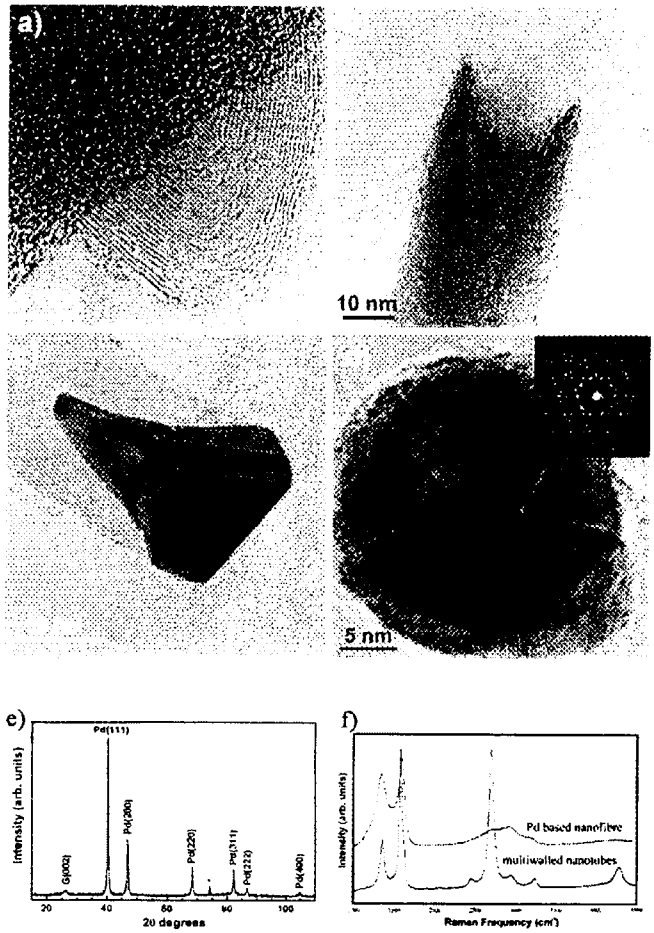

FIGURE 5 (a) TEM image of a nanofibre showing a closed conical tip, which is located on the opposite side of the Pd catalyst; (b) a nanofibre tip that lost the Pd catalyst particle, possibly by sonication treatment (see the conical interior); (c) TEM image of a conical nanofibre exhibiting a Pd 'conical' particle, which shows twinning in the interior (d) Pd decahedral cluster with five fold symmetry (inset shows the ED pattern of this particle); (e) X-ray powder diffraction pattern of the whole sample. The graphite 002 distance corresponds to 3.42 Å and the Pd corresponds to FCC Pd with a lattice parameter of 3.89 Å; (f) Raman spectrum of the whole sample showing typical graphitic features and the presence of disorder. For comparison, a highly ordered sample of multiwalled carbon nanotubes obtained by pyrolysis of ferrocene is shown.

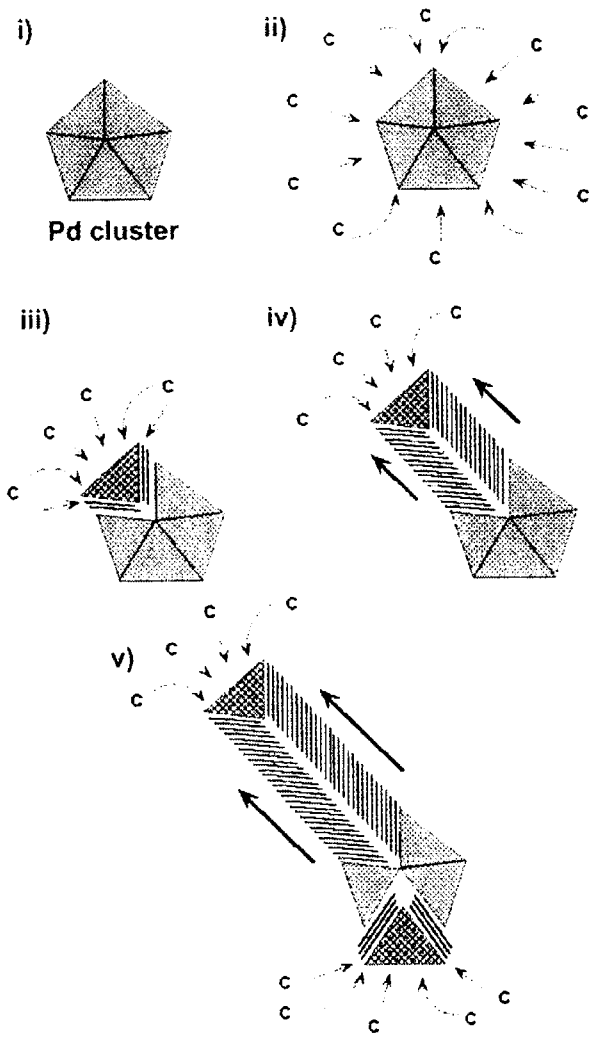

FIGURE 6 Possible growth mechanism for the conical nanofibres: (i) Pd clusters form and aggregate in order to create multiple-twinned particles (decahedral or icosahedral, see also Fig. 4d); (ii) carbon species interact with the hot Pd polygonal cluster and diffuse along the exposed surface and between the grain boundaries, thus fragmenting the twin crystals into tetrahedral-like and diamond-shaped Pd particles; (iii) carbon diffuses, on the exposed conical Pd particles, and precipitates at the other end, thus forming graphite cones; (iv–v) carbon continues to diffuse, creating 'fresh' cones, which displace the previously formed cones by releasing stress between the cones and the Pd particle, thus creating the conical fibres (See Color Plate V).

with the hot Pd polygonal cluster and diffuse along the exposed surface and between the grain boundaries, thus fragmenting the twin crystals into tetrahedral-like and diamond-shaped Pd particles; (iv) carbon diffuses, on the exposed conical Pd particles, and precipitates at the other end, thus forming graphite cones; (v) carbon continues to diffuse, creating 'fresh' cones, which displace the previously formed cones by releasing stress between the cones and the Pd particle; (vi) the carbon aggregation continues and the conical fibre is created (Fig. 6).

A decahedral Pd (D_{5h}) twin can be formed by introducing 10 distorted Pd tetrahedral crystals, and an icosahedral (I_h) twin should possess 20 of these tetrahedral [20]. In this context, the Pd catalyst initial shape might be related to these tetrahedral crystals whose faces and sharp edges are suitable for carbon diffusion, thus forming the graphene layers that mimic the catalyst particle creating cones (note that Pd is reluctant to form stable carbides and the diffusion is likely to occur just on the surface). Subsequent carbon deposition will cause the formation of additional cones, which will push the particle up, building in this way the fibre (Fig. 4). We believe that a reshaping of the catalytic particle during the growth process occurs because the exposed surface always exhibits round morphologies, whereas the interior is faceted, perhaps due to the temperature gradient.

ED (electron diffraction) direct measurements using HRTEM micrographs and FFT (fast Fourier transform) patterns from different regions of the fibres, indicate that the distance between graphene layers varies from 3.38 Å to 3.54 Å (average value of 3.45 Å, which is close to that of turbostratic graphite). On some occasions, the (100) planes of graphite can be distinguished ($d_{(100)} = 0.21$ nm).

We have identified the composition of the metal particles using ED, EDX and X-ray powder diffraction techniques. The results clearly indicate the presence of Pd (Fig. 5e) since the observed structure is similar to that of bulk Pd (FCC; lattice parameter of 3.89 Å). ED studies from these Pd particles exhibit different crystallographic orientations: the [110], [100] and [111] zone axes were identified as well as other arbitrary orientations. ED patterns show that graphitic {002} planes can be parallel to the {111}, {020} and {002} Pd planes. This observation indicates that a preferred orientation of the Pd planes with respect to the graphite {002} does not take place.

Electron energy loss spectra (EELS) on the conical nanofibres reveal typical features of sp^2 carbon, thus confirming their "graphite" nature. The Raman spectrum exhibits the characteristic features of graphitic structures, with a G-peak centered at 1598.2 cm^{-1} (1582.1 cm^{-1} for ordered multi-walled CNT obtained by pyrolysis of ferrocene [21], see Fig. 4f) and the D-peak at 1348.2 cm^{-1} (1352.5 cm^{-1} for ordered MWCNT obtained by pyrolysis of ferrocene [21]). The intensity ratio R (I_D/I_G) in our samples is *ca.* 0.847 (0.338 for highly MWCNTs obtained by pyrolysis of ferrocene [21],

though this value can be lowered by the spray pyrolysis method to ~0.232 [21]). These results indicate that the concentric graphene cones of the fibres possess more disorder (*e.g.* lack of straightness in the graphene layer) when compared to other MWCNTs obtained by pyrolysis. Heat treatment at high temperatures (2500°C), will certainly enhance the straightness of the graphene conical layers and will decrease the I_D/I_G ratio.

CONCLUSION

Conical graphitic nanofibres have been synthesized by pyrolysing three different carbon contained palladium precursors in the temperature range 850–1000°C. All of them exhibit stacked-cone shape fibres with palladium conical particles, firmly fixed, at their tips. The absence of nested cylindrical carbon nanotubes is also noteworthy. In these fibres, the shape of the graphene layers is imposed by the shape of the catalytic particle. The conical angles observed in our study can be explained by invoking an open cone approach, which provides more possibilities for illustrating the structure of graphitic cones. The cones within the fibres are held together by van der Waals forces acting between the graphene layers.

We envisage that these fibres may behave as stable field emitters operating at low voltages. Moreover, by using heavy grinding of this material, it may be possible to fragment the fibres into smaller cones. The structures also exhibit compartments between cones which may be advantageous for gas storage. Palladium metal has proved to be useful for H_2 storage; therefore, the metal at the tips may well enhance the H_2 absorption. Theoretical predictions on these novel lamp-shade fibres may reveal intriguing electronic and magnetic effects. Moreover, this technique can be also used to generate Pd clusters with a determined shape and morphology, which may be advantageous in catalysis.

REFERENCES

[1] Iijima, S. (1991). *Nature* (London), *354*, 56.
[2] Bockrath, M., Cobden, D. H., McEuen, P. L., Chopra, N. G., Zettl, A., & Smalley, R. E. (1997). *Science*, *275*, 1922.
[3] Tans, S. J., Verschueren, A. R. M., & Dekker, C. (1998). *Nature* (London), *393*, 49.
[4] Kwon, Y.-K., Tománek, D., & Iijima, S. (1999). *Phys. Rev. Lett.*, *82*, 1470.
[5] Ebbesen, T. W. (1996). *Phys. Today*, *49*(6), 26.
[6] Yakobson, B. I. & Smalley, R. E. *Am. Sci.*, *83*, 324.
[7] Kroto, H. W., Heath, J. R., O'Brien, S. C., Curl, R. F., & Smalley, R. E. (1985). *Nature*, *318*, 162.
[8] Ugarte, D. (1992). *Nature* (London), *359*, 707.
[9] Liu J. J., Dai, H. J., Hafner, J. H., Colbert, D. T., Smalley, R. E., Tans, S. J., & Dekker, C. (1997). *Nature* (London), *385*, 780.

[10] Saito, Y. & Matsumoto, T. (1998). *Nature* (London), *392*, 237.
[11] Ge, M. & Sattler, K. (1994). *Chem. Phys. Lett.*, *220*, 192.
[12] Krishnan, A., Dujardin, E., Treacy, M. M. J., Hugdahl, J., Lynum, S., & Ebbesen, T. W. (1997). *Nature* (London), *388*, 451.
[13] Iijima, S., Yudasaka, M., Yamada, R., Bandow, S., Suenaga, K., Kokai, F., & Takahashi, K. (1999). *Chem. Phys. Lett.*, *309*, 165.
[14] Berber, S., Kwon, Y.-K., & Tománek, D. (2000). *Phys. Rev. B*, *62*, R229.
[15] Lammert, P. E. & Crespi, V. H. (2000). *Phys. Rev. Lett.*, *85*, 5190.
[16] Rignanese, M.-G. & Charlier, J.-C. (2001). *Phys. Rev. Lett.*, *86*, 5970.
[17] Nakada, K., Fujita, M., Dresselhaus, G., & Dresselhaus, M. (1996). *Phys. Rev. B*, *54*, 17954.
[18] Terrones, M., Terrones, H., Grobert, N., Hsu, W. K., Zhu, Y. Q., Kroto, H. W., Walton Ph. Kohler-Redlich, D. R. M., Rühle, M., Zhang, J. P., & Cheetham, A. K. (1999). *Appl. Phys. Lett.*, *75*, 3932.
[19] Terrones, H., Hayashi, T., Muñoz-Navia, M., Terrones, M., Kim, Y. A., Grobert, N., Kamalakaran, R., Dorantes-Dávila, J., Escudero, R., Dresselhaus, M. S., & Endo, M. (2001). *Chem. Phys. Lett.*, *343*, 241.
[20] Mackay, A. L. (1962). *Acta Cryst.*, *15*, 916.
[21] Kamalakaran, R., Terrones, M., Seeger, T., Kohler-Redlich, Ph., Rühle, M., Kim, Y. A., Hayashi, T., & Endo, M. (2000). *Appl. Phys. Lett.*, *77*, 3385.